Journal of Microbiology (2017) Vol. 55, No. 5, pp. 388–395
DOI 10.1007/s12275-017-7053-8
eISSN 1976-3794
pISSN 1225-8873

Crystal structure of *Streptomyces coelicolor* RraAS2, an unusual member of the RNase E inhibitor RraA protein family

Nohra Park[1], Jihune Heo[2], Saemee Song[1], Inseong Jo[1], Kangseok Lee[2*], and Nam-Chul Ha[1*]

[1]*Department of Agricultural Biotechnology, Center for Food Safety and Toxicology, Research Institute for Agriculture and Life Sciences, Seoul National University, Seoul 08826, Republic of Korea*
[2]*Department of Life Science, Chung-Ang University, Seoul 06974, Republic of Korea*

(Received Feb 3, 2017 / Revised Apr 4, 2017 / Accepted Apr 6, 2017)

Bacterial ribonuclease E (RNase E) plays a crucial role in the processing and decay of RNAs. A small protein named RraA negatively regulates the activity of RNase E via protein-protein interaction in various bacteria. Recently, RraAS1 and RraAS2, which are functional homologs of RraA from *Escherichia coli*, were identified in the Gram-positive species *Streptomyces coelicolor*. RraAS1 and RraAS2 inhibit RNase ES ribonuclease activity in *S. coelicolor*. RraAS1 and RraAS2 have a C-terminal extension region unlike typical bacterial RraA proteins. In this study, we present the crystal structure of RraAS2, exhibiting a hexamer arranged in a dimer of trimers, consistent with size exclusion chromatographic results. Importantly, the C-terminal extension region formed a long α-helix at the junction of the neighboring subunit, which is similar to the trimeric RraA orthologs from *Saccharomyces cerevisiae*. Truncation of the C-terminal extension region resulted in loss of RNase ES inhibition, demonstrating its crucial role. Our findings present the first bacterial RraA that has a hexameric assembly with a C-terminal extension α-helical region, which plays an essential role in the regulation of RNase ES activity in *S. coelicolor*.

***Keywords*:** Rnase ES inhibitor, crystal structure, *Streptomyces coelicolor*

Introduction

Diverse RNA transcripts are processed or degraded by endoribonuclease RNase E in bacteria and higher plants; thus, RNase E is essential for their survival (Cohen and McDowall, 1997; Lee and Cohen, 2003). It is well known that RNase E in *Escherichia coli* is involved in mRNA decay, tRNA processing, and the antisense regulation of ColE1-type plasmid replication (Cohen and McDowall, 1997; Li and Deutscher, 2002; Lee *et al.*, 2003). RNase E from *E. coli* consists of a highly conserved N-terminal domain for catalysis and a C-terminal unstructured region that serves as a scaffold for RNA degradosome complex assembly (Ghora and Apirion, 1978; Callaghan *et al.*, 2004; Gorna *et al.*, 2010). The cellular amount and activity of RNase E are tightly regulated depending on cellular physiological conditions. In particular, RNase E is differentially regulated by the proteinaceous inhibitors RraA and RraB, which stand for regulator of ribonuclease activity A and B, respectively (Yeom *et al.*, 2008).

RraA requires the C-terminal unstructured region of RNase E for high affinity binding, while RraB binds to the C-terminal region to inhibit ribonucleolytic activity (Ghora and Apirion, 1978; Lee *et al.*, 2003; Gao *et al.*, 2006, Seo *et al.*, 2017). Globally, these inhibitors govern the transcript levels of various genes by modulating the functional activity of RNase E in many bacteria (Lee *et al.*, 2003). Numerous orthologs of *E. coli* RraA have been found, including RraAV1 and RraV2 in *Vibrio vulnificus*, RraA in *Pseudomonas aeruginosa*, and RraAS1 and RraAS2 in *Streptomyces coelicolor* (Lee and Cohen, 2003; Lee *et al.*, 2009; Tang *et al.*, 2010; Heo *et al.*, 2016; Kim *et al.*, 2016; Seo *et al.*, 2017).

The gram-positive bacterium *S. coelicolor* contains two RNase E-like enzymes, one of which is designated RNase ES (Lee and Cohen, 2003). RNase ES of *S. coelicolor* (simply called RNase ES in this study) has three distinct regions. The central domain and the C-terminal region of RNase ES exhibit high sequence similarities to the catalytic domain and the C-terminal unstructured region of RNase E of *E. coli*, respectively (Lee and Cohen, 2003). The additional N-terminal extension region of RNase ES is also analogous to the C-terminal unstructured region. The inhibitory proteins RraAS1 and RraAS2 of *S. coelicolor* are ~ 60 amino acids longer than typical RraA proteins found in other bacteria (Lee and Cohen, 2003; Lee *et al.*, 2009; Kim *et al.*, 2016). In particular, RraAS2 has a lower sequence similarity (37% sequence identity) to RraA of *E. coli* than does RraAS1.

The crystal structure of *E. coli* RraA was determined, revealing a ring-like homotrimeric assembly with a central cavity 12 Å in diameter (Monzingo *et al.*, 2003). Interestingly, RraA from *P. aeruginosa* forms a hexamer arranged in a dimer of trimers, indicating structural diversity in the oligomeric state of RraA proteins (Tang *et al.*, 2010). The RraA family protein Yer010cp from *Saccharomyces cerevisiae* displayed a trimeric structure with 4-hydroxy-4-methyl-2-oxoglutarate (HMG) aldolase and oxaloacetate decarboxylase activities (Leulliot *et al.*, 2005; Mazurkewich *et al.*, 2014). The *S. cerevisiae* protein has a longer C-terminal region similar to the RraA proteins of *S. coelicolor*. Here, we present the crystal structure

*For correspondence. (K. Lee) E-mail: kangseok@cau.ac.kr; Tel.: +82-2-820-5241; Fax: +82-2-825-5206 / (N.-C. Ha) E-mail: hanc210@snu.ac.kr; Tel: +82-2-880-4853; Fax: +82-2-873-5095

of RraAS2 from *S. coelicolor* and establish a role for the C-terminal extension region of the protein.

Materials and Methods

Cloning and protein purification

To express the full-length RraAS2, we used pET15b-RraAS2, which was described previously (Heo *et al*., 2016). For expression of a truncation mutant (residues 1–220), the corresponding region was amplified by PCR using pET15b-RraAS2 as a template. The PCR products were inserted into the expression vector pET15b (Invitrogen, USA) using restriction enzyme sites *Nde*I/*Bam*HI, resulting in pET15b-RraAS2ΔC. The resulting plasmids were used to transform *E. coli* BL21 (DE3) for protein expression. *E. coli* BL21(DE3) harboring the expression plasmid was cultured in 3 L of LB medium including appropriate antibiotics until the OD_{600} reached about 0.4, at which time protein expression was induced with 0.5 mM IPTG at 30°C. For the production of the selenomethionine (SeMet)-labeled protein, pET15b-RraAS2 was used to transform the *E. coli* B834 (DE3) strain, and the cells were cultured in M9 medium in the presence of L-selenomethionine. After induction, cells were harvested for 6 h for the culture in LB medium or 12 h for the culture in M9 medium. Then the cell pellet was resuspended with 100 ml lysis buffer containing 20 mM Tris-HCl (pH 8.0), 300 mM NaCl, and 2 mM 2-mercaptoethanol. After the cells were homogenized by French-press at 20 kpsi, the cell lysate was acquired by centrifugation at 13,000 rpm for 30 min. The proteins were subsequently purified using Ni-NTA affinity chromatography (Invitrogen) and anion-exchange chromatography (HiTrap Q, GE Healthcare). Then, the proteins were further purified by size exclusion chromatography (HiLoad Superdex 200 26/600; GE Healthcare), pre-equilibrated with lysis buffer. The final protein samples were concentrated to 11 mg/ml using a centrifugal filter concentration device (Millipore; 10 kDa cutoff) and stored frozen at -80°C until use.

Crystallization, data collection, and structural determination

Crystallization of the native RraAS2 protein was performed by the vapor-diffusion hanging drop method at 14°C under a mother liquor containing 0.1 M NaCl, 0.1 M bis-Tris propane (pH 8.5), and 19% (*w*/*v*) PEG 1500. For the SeMet-labeled crystals, the SeMet-labeled RraAS2 protein was applied to the same conditions as used in the native RraAS2 protein. The crystals were flash-frozen using Paratone-N as a cryoprotectant under a nitrogen stream at -173°C prior to collecting the dataset. X-ray diffraction datasets were collected at the 5C beamline in of the Pohang Accelerator Laboratory (Park *et al*., 2017) and processed with the HKL2000 package (Otwinowski and Minor, 1997). Both native and SeMet-labeled crystals belong to the $P3_221$ space group with similar unit cell dimensions (Table 1). The structure was determined with the single anomalous dispersion (SAD) method using the dataset from the SeMet-labeled crystal and the PHENIX program (Adams *et al*., 2010). The model was built using the COOT program (Emsley *et al*., 2010). The final structure of RraAS2 was refined at a 3.1 Å resolution with an R_{factor} of 26% and an R_{free} of 32% using the PHENIX program (Adams *et al*., 2010). Further details on structure determination and refinement are given in Table 1.

Analytical size exclusion chromatography

To estimate the oligomeric state of the protein, size exclusion chromatography was carried out using a Superdex 200 10/300 GL column (GE Healthcare). The protein sample was applied to the column pre-equilibrated with 20 mM Tris buffer (pH 8.0) containing 150 mM NaCl and 2 mM 2-mercaptoethanol. The following size standard proteins were used: ferritin (440 kDa), aldolase (158 kDa), conalbumin (75 kDa), ovalbumin (44 kDa), carbonic anhydrase (29 kDa), and RNase A (13.7 kDa). The void volume of the column was measured with Blue Dextran (GE Healthcare). Peak elution volumes were used for the calculation of the standard curve deduced from the standard proteins.

Measurement of plasmid copy number

The procedure used for measuring plasmid copy number was described previously (Lee and Cohen, 2003). This study employed *E. coli* strain KSL2005 cells that expressed full-length RNase ES in a plasmid pRNES101, whose copy number is independent of RNase E or RNase ES. The KSL2005 cells were transformed with ColE-type plasmid pKAN6B,

Table 1. Statistics for X-ray data collection and refinement

	Native	SeMet
Data collection		
Beamline	PAL 5C	PAL 5C
Wavelength (Å)	1.2823	0.97940
Space group	$P3_221$	$P3_221$
Cell dimensions		
a,*b*,*c* (Å)	96.9, 96.9, 166.6	99.5, 99.5, 166.9
α,β,γ (°)	90, 90, 120	90, 90, 120
Resolution (Å)	50–3.1 (3.15–3.10)	50–3.4 (3.46–3.40)
R_{merge}	0.084 (0.351)	0.056 (0.251)
$I/\sigma I$	36.4 (2.1)	22.33 (3.3)
Completeness (%)	98.3 (98.6)	96.5 (89.5)
Redundancy	8.6 (4.8)	9.0 (3.3)
Refinement		
Resolution (Å)	48.46–3.10	
No. of reflections	13795	
R_{work}/R_{free}	0.26/0.32	
No. of total atoms	4556	
Wilson B-factor (Å)	56.1	
RMSD		
Bond lengths (Å)	0.003	
Bond angles (°)	0.644	
Ramachandran plot		
Favored (%)	90.22	
Allowed (%)	8.40	
Outliers (%)	1.37	
PDB ID	5×15	

*Values in parentheses are for the highest-resolution shell
**$R_{merge} = \Sigma_{hkl}\Sigma_i|I_i(hkl) - [I(hkl)]|/\Sigma_{hkl}\Sigma_i I_i(hkl)$, where $I_i(hkl)$ is the intensity of the *i*th observation of reflection *hkl* and [I(*hkl*)] is the average intensity of the *i* observations
***R_{free} calculated for a random set of 10% of reflections not used in the refinement

pKAN6B-RraAS2, or pKAN6B-RraAS2ΔC to express null, full-length RraAS2, or RraAS2ΔC, respectively. The cells were cultured in LB medium containing 10 μM IPTG for the basal expression of RNase ES. When the cell culture reached an OD_{600} of 0.1, the cells were treated with 1 mM IPTG and 0.2% arabinose and further grown to an OD_{600} of 1.0. The obtained plasmids from the cells were digested with restriction enzymes *Afl*II and *Hin*dIII, corresponding to the unique sites in pRNES101, as well as pKAN6B, pKAN6B-RraAS2, and pKAN6B-RraAS2ΔC. The digested plasmids were measured by electrophoresis in a 0.9% (*w*/*v*) agarose gel and stained with ethidium bromide. The plasmid copy number was calculated relative to concurrently present pRNES101 by measuring the molar ratio of pRNES101 to the ColE1-type plasmid (pKAN6B, pKAN6B-RraAS2, or pKAN6B-RraAS2ΔC).

RNA preparation and reverse transcriptase (RT)-PCR

Total RNA was isolated using an RNeasy Miniprep Kit (Qiagen) from KSL2005 pKAN6B, pKAN6B-RraAS2, or pKAN6B-RraAS2ΔC cells grown to an OD_{600} of 0.1 containing 10 μM IPTG, and 1 mM IPTG and 0.2% (*w*/*v*) arabinose were added. Synthesis of *ftsZ* cDNA was performed using the PrimeScript First-strand cDNA Synthesis Kit system for RT-PCR (Takara), according to the manufacturer's instructions. For RT-PCR, 2 μg of total RNA and *ftsZ* specific primers *ftsZ* 3'RT were used in each reaction (Heo *et al.*, 2016).

In vitro RNase ES assay

The *in vitro* RNase E cleavage assay using RNase ES from *S. coelicolor* was previously described (Heo *et al.*, 2016). Briefly, a synthetic transcript (BR10+hpT) was radiolabeled at the 3' end using [γ-^{32}P] ATP and T4 polynucleotide kinase (Takara). The labeled product, called p-BR10+hpT, was purified using MicroSpin TM G25 columns (GE Healthcare). At the preincubation step, p-BR10+hpT (0.5 pmol) was incubated with the full-length RNase ES (0.3 pmol) at full-length or truncated RraAS2 (30 and 120 pmol) protein on ice for 10 min in 20 μl of 200 mM Tris buffer (pH 8.0) containing 1 M NaCl, 1 mM DTT, 50 mM $MgCl_2$, and 50% (*v*/*v*) glycerol. At the main reaction step, the reaction proceeded at 37°C for 2 h. The samples were mixed with an equal volume of loading buffer and then denatured at 65°C for 5 min. The final products were separated on a 12% denaturing polyacrylamide gel containing 8 M urea. The percentage of uncleaved p-BR10+hpT in the gel was measured using a phospho-imager and OptiQuant software.

Results

Structural determination and overall structure of RraAS2

We purified the full-length RraAS2 protein from *S. coelicolor* using an *E. coli* expression system. The resulting protein contains a hexahistidine tag at the N-terminus, and the protein was successfully crystallized at pH 8.5. The structure of the RraAS2 protein was determined at a 3.1 Å resolution by single anomalous diffraction (SAD) using SeMet-substituted crystals (Table 1). The asymmetric unit contained three molecules, and the packing analysis indicated one homotrimeric unit in the asymmetric unit (Fig. 1A). Three protomers associate as a doughnut-shaped arrangement showing a 76 Å outer diameter and a 12 Å inner diameter (Fig. 1B).

Sequence comparison suggested that RraAS2 consists of a core conserved domain (residues 1-220) and a C-terminal extension region (residues 221-270) (Fig. 1C). In the core conserved domain, RraAS2 showed 30% and 34% amino acid sequence identity with *E. coli* RraA and *P. aeruginosa* RraA, respectively. RraA homologs from *Saccharomyces cerevisiae* and *Candida albicans* possess this C-terminal extension region as well (Monzingo *et al.*, 2003), indicating that the RraAS2 of *S. coelicolor* likely shares structural features with such RraA homologs (Ahn *et al.*, 2008). The RraAS2

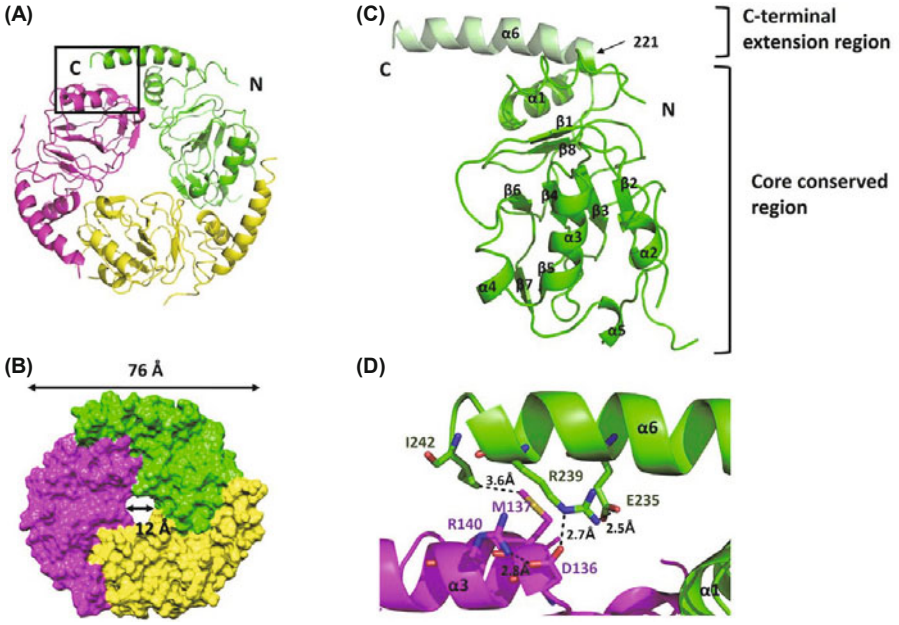

Fig. 1. Overall structure of RraAS2. (A) Ribbon representation of the asymmetric unit. Each protomer is differently colored. The both terminus were labeled as 'N' and 'C'. (B) Surface representation of RraAS2 with approximate molecule dimensions. The outer and inner diameters are presented with dihedral arrow lines, respectively. (C) The protomer structure. Each secondary structure element is labeled. The core conserved region is in green, and the C-terminal extension region is in pale green. (D) Inter-subunit interaction involved in the C-terminal extension region, which is boxed in Fig.1A.

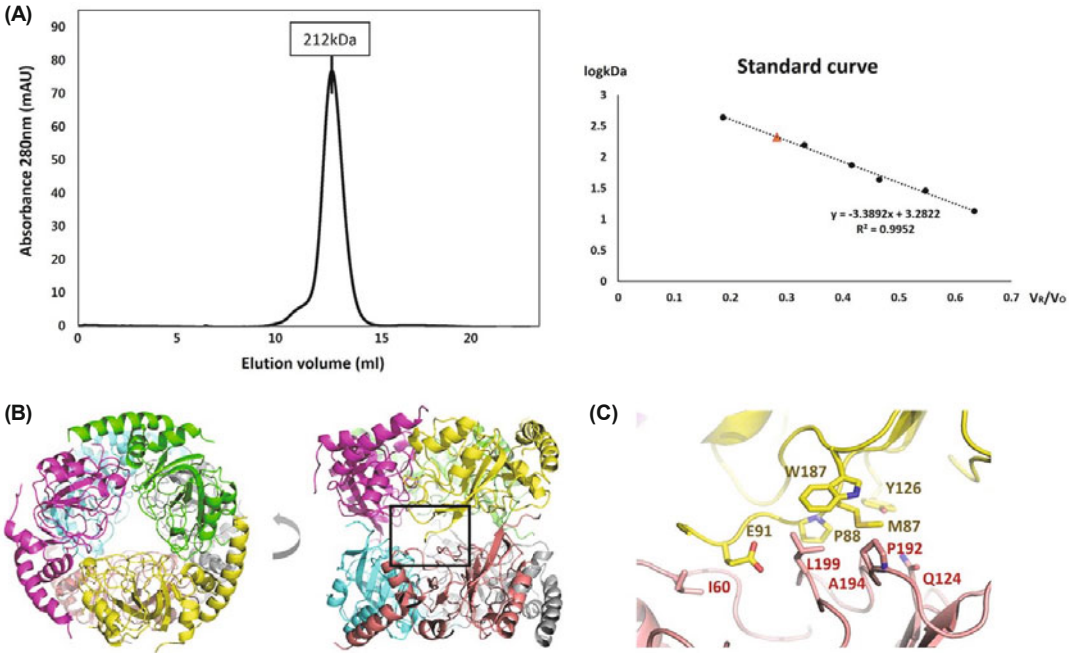

Fig. 2. Hexameric structure of RraAS2. (A) Elution profile of the full-length RraAS2 protein on a size exclusion chromatographic column (*left*). The calculated molecule size of the protein in solution is labeled on the peak, based on the following standard proteins: ferritin (440 kDa), aldolase (158 kDa), conalbumin (75 kDa), ovalbumin (44 kDa), carbonic anhydrase (29 kDa), and RNase A (13.7 kDa). The standard curve was shown (*right*) and the red triangle represents the full-length RraAS2. Plotting of the logarithm of the molecular weight (logkDa) for each standard protein was done as a function of the ratio of the protein retention volume (V_R) to the column void volume (Vo). (B) Hexameric RraAS2 crystal structure from the top view (*left*) and the side view (*right*). The box indicates the interaction between the two dimers. Each protomer is colored differently. (C) Magnified view of the hexameric assembly interface, which is boxed in Fig. 2B. The residues and numbers are labeled with the same color used in the corresponding subunits.

monomer consists of 5 α-helices and 6 β-strands in the core conserved domain, which consists of three layers of β-sheets that tightly pack against each other through extensive hydrophobic interactions, similar to the structure of other RraA-like proteins (Monzingo *et al*., 2003; Leulliot *et al*., 2005). The C-terminal extension region forms an additional structural motif, protruding from the core domain. The C-terminal extension region consists of a loop followed by an α-helix (α6), which decorates the outer region of the core conserved domain with the inter-subunit interaction of the protein.

Homotrimerization interactions

As observed in RraA from *E. coli*, the core conserved domain also seems to be involved in homotrimerization with the loops connecting β1-β2, β11-β12, and β8-β9 from the other inter-subunit. The α-helix at the C-terminal extension region seems to be more important in trimer formation because it is anticipated to bond with Met137, Asp136, and Arg140 on the adjacent subunit chain (Fig. 1D).

Hexameric assembly

Size exclusion chromatography showed that the protein behaved as a homohexamer in solution, which is consistent with the crystal packing analysis (Fig. 2A). The trimer has top and bottom faces, with the top face containing the C-terminal extension α6 helix. Two trimers in the RraAS2 hexamer face each other at the bottom faces. The two trimer units in the hexamer do not rotate through the 3-fold of the trimer (Fig. 2B). To form the hexamer from two trimers, Met87, Pro88, Glu91, Tyr126, and Trp187 of the upper trimer unit make contact with Ile60, Gln124, Pro192, Ala194, and Leu199 of the lower trimer unit, respectively (Fig. 2C). In the hexameric structure of *P. aeruginosa* RraA, the two trimers interact with one another at the bottom faces, similar to RraAS2; however, the trimers rotate about 45° through the axis of the 3-fold of the trimer in *P. aeruginosa* RraA (Tang *et al*., 2010). The contacting residues that mediate hexamerization by the two trimers are also different from those in RraAS2.

Structural comparison with other RraA proteins

We performed a sequence alignment with RraA family proteins whose crystal structures were known: RraA from *E. coli* (PDB code 1Q5X), TTHA1322 from *Thermus thermophilus* (PDB code 1J3L), Rv3853 from *Mycobacterium tuberculosis* (PDB code 1NXJ), VC2366 from *Vibrio cholerae* (PDB code 1VI4), and Yer010cp from *S. cerevisiae* (PDB code 2C5Q) (Monzingo *et al*., 2003; Rehse *et al*., 2004; Badger *et al*., 2005; Leulliot *et al*., 2005) (Fig. 3A). The amino acid sequence identity and the root mean square deviation (RMSD) in the core conserved regions between RraAS2 and the other proteins are listed in Table 2. Most structures were similar in the core conserved regions; however, Yer010cp from *S. cerevisiae* showed the narrowest inner channel (Fig. 3B).

Unlike typical bacterial RraA proteins, the C-terminal extension region is present in Yer010cp from *S. cerevisiae* and RraAS2 from *S. coelicolor* (Fig. 3B and 3C). In the Yer010cp

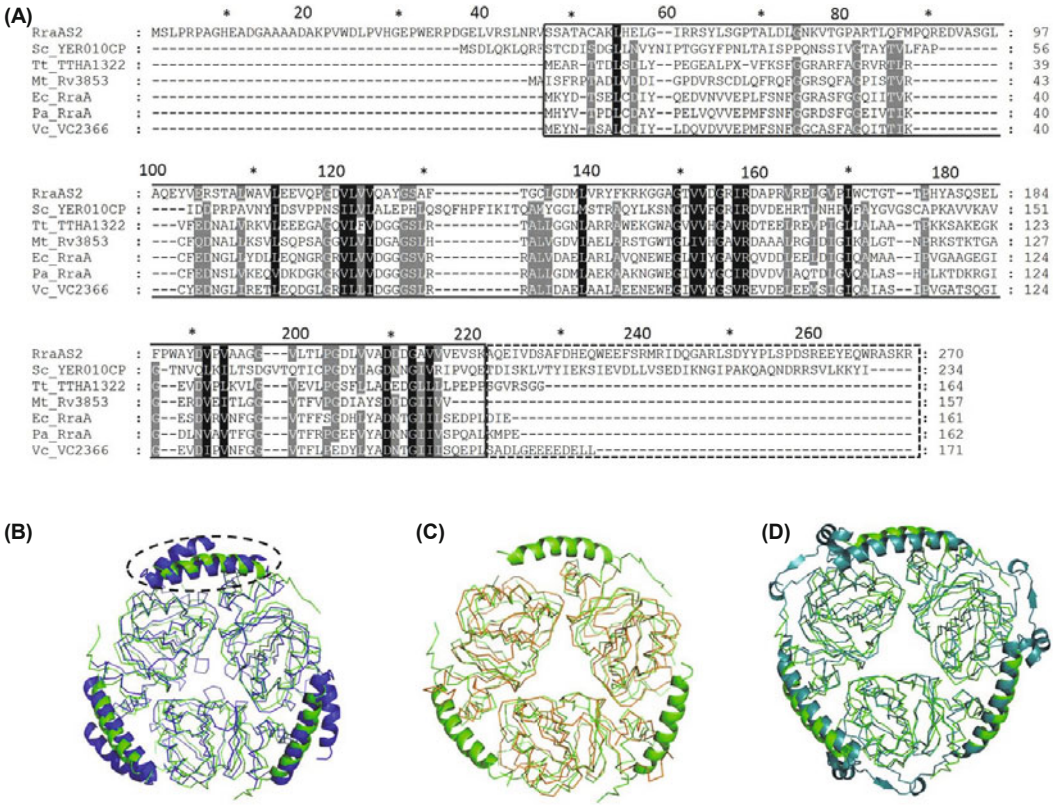

Fig. 3. Alignment of RraAS2 with homologs. (A) Sequence alignment of the RraA family proteins whose structures are available. Sc_YER010CP, Yer010cp from *S. cerevisiae*; Tt_TTHA1322, TTHA1322 from *T. thermophilus*; Mt_Rv3853, Rv3853 from *M. tuberculosis*; Ec_RraA, RraA from *E. coli*; Pa_RraA, RraA from *P. aeruginosa*; and Vc_VC2366, VC2366 from *V. cholerae*. The core conserved domain and the C-terminal extension region are separately displayed by solid and dash-lined boxes, respectively. The number above the aligned sequence is based on RraAS2. (B) Structural superposition of RraAS2 from *S. coelicolor* (green) and Yer010cp from *S. cerevisiae* (blue). (C) Structural superposition of RraAS2 (green) onto TTHA1322 from *T. thermophilus* (orange). (D) Structural superposition of RraAS2 (green) onto HMG/CHA aldolase from *Pseudomonas putida* F1 (deep teal). The core domain is displayed as a Cα tracing, and the C-terminal region is represented by the ribbon representation.

structure, two long α-helices are in the C-terminal extension region, unlike RraAS2, which has only one α-helix in the C-terminal extension region. The two α-helices in Yer010cp were suggested to stabilize homotrimerization, although no biochemical evidence was presented to support this (Monzingo *et al.*, 2003).

Structural comparison of RraAS2 and HMG/CHA aldolase

The HMG/4-carboxy-4-hydroxy-2-oxoadipate (CHA) aldolase is a class II pyruvate aldolase which requires divalent metal ion (Mazurkewich *et al.*, 2014). The crystal structure of HMG/CHA aldolase from *Pseudomonas putida* F1 has been identified (PDB code 3NOJ) (Mazurkewich *et al.*, 2014).

Table 2. Structural comparison of RraAS2 to structural homologs

	Sequence identity	RMSD between Cα atoms of matched residues
Tt TTHA1322	36%	1.249 (108 to 108 atoms)
Mt Rv3853	35%	1.363 (109 to 109 atoms)
Sc YER010CP	29%	1.733 (90 to 90 atoms)
Ec RraA	30%	1.237 (101 to 101 atoms)
Pa RraA	34%	1.147 (86 to 86 atoms)
Vc VC2366	26%	1.249 (83 to 83 atoms)

Like RraA family proteins, the core domain of the aldolase consists of αββα sandwich fold which is different from other class II pyruvate aldolase. RraAS2 and *P. putida* F1 HMG/CHA aldolase are shared in the hexameric assembly and the C-terminal extension despite low sequence identity (28%) (Fig. 3D).

Putative active site

A notable pocket corresponding to the active site of *P. putida* F1 HMG/CHA aldolase was found in the core conserved domain at the interface between the core region and the α-helix in the C-terminal extension region of the neighboring monomer (Fig. 4). The pocket is lined with residues Ser47, Ala49, Thr50, Arg157, Asp158, and Arg161 in the core conserved region, which are mostly conserved among RraA family members (Fig. 4). Interestingly, Arg157 and Asp158 was known to be necessary for the enzyme activity in the active site of *P. putida* F1 HMG/CHA aldolase (Mazurkewich *et al.*, 2014). The C-terminal helix serves as a lid for the pocket in the RraAS2 structure because Glu232, Glu235, and Arg239 in the C-terminal helix are located in the putative active site. These findings indicate that the pocket may be related to the function of RraAS2, although further study is required to validate this function.

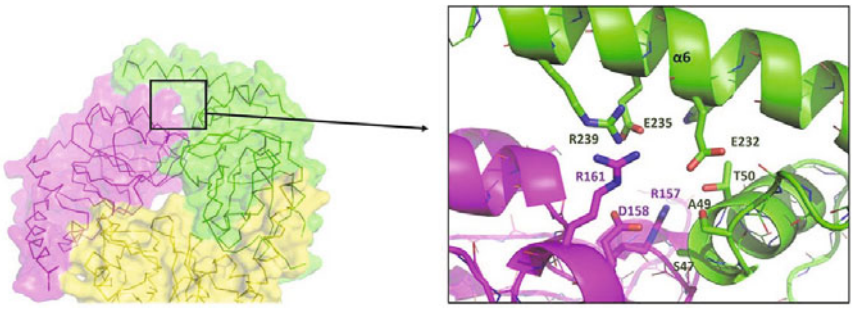

Fig. 4. Putative active site pocket. The active site pocket is located at the interface between the protomers, which is shown in the surface representation and is differently colored in each domain. The residues lined with the pockets are enlarged and displayed in the stick representation in the inset.

Function of the C-terminal extension region

To determine the function of the C-terminal extension region, we generated a truncation mutant of RraAS2 that is devoid of the C-terminal extension region, called RraAS2ΔC. The RraAS2ΔC protein was expressed in the *E. coli* cytosol, indicating structural integrity of the protein. To compare the inhibitory RNase ES ribonucleolytic activity function of the full-length and mutant RraAS2 in *in vivo*, we co-expressed the full-length and mutant RraAS2 proteins in pKAN6B plasmids with the ColE1-type origin in the *E. coli* strain KLS2005 (Heo *et al*., 2016). The strain KLS2005 contains the pSC101-derived plasmid pRNES101 expressing RNase ES from *S. coelicolor* in the RNase E-deleted background (Lee and Cohen, 2003). In this system, the RraAS2 proteins were induced by arabinose, while RNase ES was induced by IPTG. We employed two methods to measure the *in vivo* activity of RNase ES. First, we assessed the *in vivo* activity of RNase ES toward RNA I, an antisense repressor of ColE1-type plasmid replication, by measuring the relative copy number of a ColE1-type plasmid (pKan6B, pKan6B-RraAS2, or pKan6B-RraAS2ΔC) to a pSC101-derived plasmid (pRNES101) when RraAS2 or RraAS2ΔC was conditionally co-expressed in *E. coli* KSL2005 cells (Fig. 5A). The ColE1-type plasmid copy number was decreased by the induction of full-length RraAS2 compared with the empty pKAN6B vector control; however, the RraAS2ΔC protein did not decrease the ColE1-type plasmid copy number as much as the full-length protein. These results indicate lower inhibitory activity of RraAS2ΔC relative to the full-length protein. Second, we measured the ri-

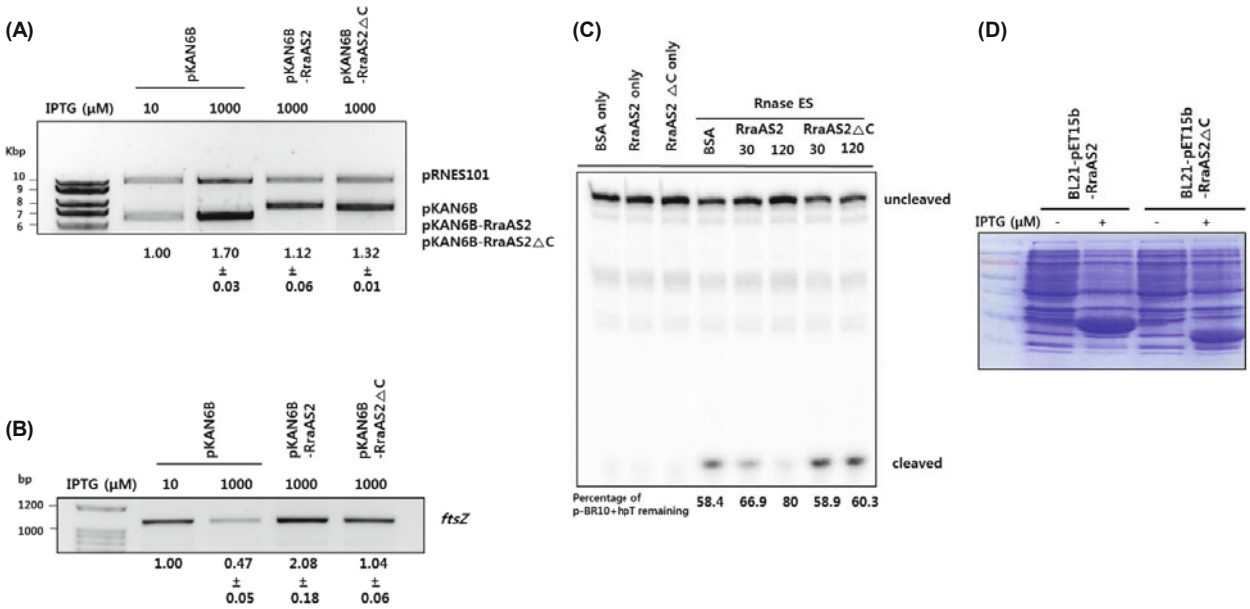

Fig. 5. The function of the C-terminal extension region of RraAS2. (A) Effects of co-expressed RraAS2ΔC on ColE1-type plasmid copy number. Plasmid copy number was calculated by measuring the molar ratio of pRNES101 to ColE1-type plasmids (pKAN6B or pKAN6B-RraAS2 or pKAN6B-RraAS2ΔC). To induce RNase ES at a basal level or at overexpression level, 10 or 1,000 μM IPTG was added to the KSL2005-based *E. coli* strains. Arabinose was added to all the strains to induce RraAS2 or RraAS2ΔC. Three independent experiments were carried out, and the standard deviations are displayed as ±. (B) Effects of co-expressed RraAS2ΔC on the steady-state level of *ftsZ* mRNA. Total RNA was isolated from KSL2005 cells grown to an OD_{600} of 1.0, and then RT-PCR was performed. The intensity of *ftsZ* mRNA was quantified from three independent experiments. (C) Autoradiogram of the radiolabeled p-BR10+hpT RNA substrate. The full-length RraAS2 and RraAS2ΔC proteins were compared for their ability to inhibit p-BR10+hpT (0.5 pmol) cleavage by RNase ES (0.3 pmol) *in vitro*. The full-length RraAS2 and RraAS2ΔC proteins were expressed and purified in the *E. coli* strain BL21(DE3) transformed with pET15b-RraAS2 or pET15b-RraAS2ΔC. RraAS2 or RraAS2ΔC was used at 30 or 120 pmol, judged by the band intensity. The percentage of uncleaved p-BR10+hpT in the gel was measured using a phosphoimager and OptiQuant software. (D) Expression level of RraAS2 and RraAS2△C. To induce the proteins, IPTG was added to the cell. The expression level of full-length RraAS2 and RraAS2ΔC proteins used in (C) was identified by SDS-PAGE.

bonucleolytic activity of RNase ES using a known RNase E substrate, *ftsZ* mRNA (Lee *et al.*, 2009), when RraAS2ΔC was co-expressed in the *E. coli* strain KSL2005 at steady-state level. The abundance of *ftsZ* mRNA was measured using semiquantitative RT-PCR (Fig. 5B). The results confirmed the reduced inhibitory effect of RraAS2ΔC on the ribonucleolytic activity of RNase ES *in vivo*.

We further confirmed the reduced inhibitory activity toward RNase ES *in vitro* (Fig. 5C) using an RNase assay performed with a radiolabeled synthetic transcript, p-BR10+ hpT, as a substrate (Heo *et al.*, 2016). Strikingly, the purified RraAS2ΔC protein completely lost inhibitory activity compared to the full-length protein (Fig. 5C).

Discussion

S. coelicolor is a soil-dwelling gram-positive bacterium belonging to the *Actinobacteria* phylum and is distinguished for its unique mycelial and sporulating life cycle, which suggests the requirement for sophisticated regulation of gene expression (Sigle *et al.*, 2015). RraAS1 and RraAS2 were identified in *S. coelicolor* as RNase ES inhibitory genes (Ahn *et al.*, 2008; Heo *et al.*, 2016). In particular, RraAS2 exerted an inhibitory effect on RNase ES, where the C-terminal scaffold domains of RNase ES are also required for tight binding to RraAS2 (Heo *et al.*, 2016). RraAS1 and RraAS2 are longer in the C-terminal extension region than other bacterial RraA family members or other homologous proteins. In this study, we determined the crystal structure of RraAS2 from *S. coelicolor*, showing a dimer of trimers arrangement. In the trimer assembly, a characteristic propeller-like structure was observed by the long α-helix, which consists of the C-terminal extension region. This C-terminal region was important for inhibiting RNase ES *in vivo* and *in vitro*. Although several lines of evidence indicate that RraA proteins directly inhibit the cognate RNase, it remains unclear how RraA interacts with the RNases.

Bacterial RraA proteins, such as *E. coli* RraA and RraAV1 and RraAV2 from *V. vulnificus*, lack the C-terminal extension region (Monzingo *et al.*, 2003; Kim *et al.*, 2016). Despite the absence of the C-terminal extension region, the bacterial RraA maintain a trimeric assembly with inhibitory activity on cognate RNases. In *P. aeruginosa* RraA, the trimeric unit further dimerizes into a hexamer like RraAS2. Most RraA homologs from fungi have a C-terminal extension region with two α-helices that have been suggested to be important for homotrimerization (Leulliot *et al.*, 2005). Interestingly, RraAS2 from the bacterium *S. coelicolor* has a C-terminal extension region that is characterized by one long α-helix. It is possible that this resemblance to fungal RraA proteins may be related to the sophisticated gene expression required in *S. coelicolor*.

In addition, we observed the remarkable structural resemblance between RraAS2 and *P. putida* F1 HMG/CHA aldolase, including the hexameric assembly and the C-terminal extension region. Furthermore, RraAS2 is likely to exhibit an enzymatic activity because of the notable pocket containing the Arg157 and Asp158 residues that are important in the catalysis of *P. putida* F1 HMG/CHA aldolase. Further study is required to see the new function of RraAS2 as an enzyme.

The findings of the present study contribute to our knowledge of the structure and functionality of RraA family proteins.

Acknowledgements

This study made use of the 5C beamline from Pohang Light Sources (Pohang, Republic of Korea). This research was supported by the R&D Convergence Center Support Program (to NCH) funded by the Ministry of Agriculture, Food, and Rural Affairs, Republic of Korea, and by the National Research Foundation of Korea (2014R1A2A2A09052791 to KL).

References

Adams, P.D., Afonine, P.V., Bunkoczi, G., Chen, V.B., Davis, I.W., Echols, N., Headd, J.J., Hung, L.W., Kapral, G.J., Grosse-Kunstleve, R.W., *et al.* 2010. Phenix: a comprehensive Python-based system for macromolecular structure solution. *Acta Crystallogr. D Biol. Crystallogr.* **66**, 213–221.

Ahn, S., Shin, E., Yeom, J.H., and Lee, K. 2008. Modulation of *Escherichia coli* RNase E activity by RraAS2, a *Streptomyces coelicolor* ortholog of RraA. *Korean J. Microbiolol.* **44**, 93–97.

Badger, J., Sauder, J.M., Adams, J.M., Antonysamy, S., Bain, K., Bergseid, M.G., Buchanan, S.G., Buchanan, M.D., Batiyenko, Y., Christopher, J.A., *et al.* 2005. Structural analysis of a set of proteins resulting from a bacterial genomics project. *Proteins* **60**, 787–796.

Callaghan, A.J., Aurikko, J.P., Ilag, L.L., Gunter Grossmann, J., Chandran, V., Kuhnel, K., Poljak, L., Carpousis, A.J., Robinson, C.V., Symmons, M.F., *et al.* 2004. Studies of the RNA degradosome-organizing domain of the *Escherichia coli* ribonuclease RNase E. *J. Mol. Biol.* **340**, 965–979.

Cohen, S.N. and McDowall, K.J. 1997. RNase E: still a wonderfully mysterious enzyme. *J. Mol. Biol.* **23**, 1099–1106.

Emsley, P., Lohkamp, B., Scott, W.G., and Cowtan, K. 2010. Features and development of Coot. *Acta Crystallogr. D Biol. Crystallogr.* **66**, 486–501.

Gao, J., Lee, K., Zhao, M., Qiu, J., Zhan, X., Saxena, A., Moore, C.J., Cohen, S.N., and Georgiou, G. 2006. Differential modulation of *E. coli* mRNA abundance by inhibitory proteins that alter the composition of the degradosome. *Mol. Microbiol.* **61**, 394–406.

Ghora, B.K. and Apirion, D. 1978. Structural analysis and *in vitro* processing to p5 rRNA of a 9S RNA molecule isolated from an rne mutant of *E. coli*. *Cell* **15**, 1055–1066.

Gorna, M.W., Pietras, Z., Tsai, Y.C., Callaghan, A.J., Hernandez, H., Robinson, C.V., and Luisi, B.F. 2010. The regulatory protein RraA modulates RNA-binding and helicase activities of the *E. coli* RNA degradosome. *RNA* **16**, 553–562.

Heo, J., Kim, D., Joo, M., Lee, B., Seo, S., Lee, J., Song, S., Yeom, J.H., Ha, N.C., and Lee, K. 2016. RraAS2 requires both scaffold domains of RNase ES for high-affinity binding and inhibitory action on the ribonucleolytic activity. *J. Microbiol.* **54**, 660–666.

Kim, D., Kim, Y.H., Jang, J., Yeom, J.H., Jun, J.W., Hyun, S., and Lee, K. 2016. Functional Analysis of *Vibrio vulnificus* Orthologs of *Escherichia coli* RraA and RNase E. *Curr. Microbiol.* **72**, 716–722.

Lee, K. and Cohen, S.N. 2003. A *Streptomyces coelicolor* functional orthologue of *Escherichia coli* RNase E shows shuffling of catalytic and PNPase-binding domains. *Mol. Microbiol.* **48**, 349–360.

Lee, K., Zhan, X., Gao, J., Qiu, J., Feng, Y., Meganathan, R., Cohen, S.N., and Georgiou, G. 2003. RraA. a protein inhibitor of RNase E activity that globally modulates RNA abundance in *E. coli*. *Cell* **114**, 623–634.

Lee, M., Yeom, J.H., Sim, S.H., Ahn, S., and Lee, K. 2009. Effects of *Escherichia coli* RraA orthologs of *Vibrio vulnificus* on the ribonucleolytic activity of RNase E *in vivo*. *Curr. Microbiol.* **58**, 349–353.

Leulliot, N., Quevillon-Cheruel, S., Graille, M., Schiltz, M., Blondeau, K., Janin, J., and Van Tilbeurgh, H. 2005. Crystal structure of yeast YER010Cp, a knotable member of the RraA protein family. *Protein Sci.* **14**, 2751–2758.

Li, Z. and Deutscher, M.P. 2002. RNase E plays an essential role in the maturation of *Escherichia coli* tRNA precursors. *RNA* **8**, 97–109.

Mazurkewich, S., Wang, W., and Seah, S.Y. 2014. Biochemical and structural analysis of RraA proteins to decipher their relationships with 4-hydroxy-4-methyl-2-oxoglutarate/4-carboxy-4-hydroxy-2-oxoadipate aldolases. *Biochemistry* **53**, 542–553.

Monzingo, A.F., Gao, J., Qiu, J., Georgiou, G., and Robertus, J.D. 2003. The X-ray structure of *Escherichia coli* RraA (MenG), A protein inhibitor of RNA processing. *J. Mol. Biol.* **332**, 1015–1024.

Otwinowski, Z. and Minor, W. 1997. Processing of X-ray diffraction data collected in oscillation mode. *Methods Enzymol.* **276**, 307–326.

Park, S., Ha, S., and Kim, Y. 2017. The protein crystallography beamlines at the pohang light source ll. *Biodesign* **5**, 30–34.

Rehse, P.H., Kuroishi, C., and Tahirov, T.H. 2004. Structure of the RNA-processing inhibitor RraA from *Thermus thermophilis*. *Acta Crystallogr. D Biol. Crystallogr.* **60**, 1997–2002.

Seo, S., Kim, D., Song, W., Heo, J., Joo, M., Lim, Y., Yeom, J.H., and Lee, K. 2017. RraAS1 inhibits the ribonucleolytic activity of RNase ES by interacting with its catalytic domain in *Streptomyces coelicolor*. *J. Microbiol.* **55**, 37–43.

Sigle, S., Ladwig, N., Wohlleben, W., and Muth, G. 2015. Synthesis of the spore envelope in the developmental life cycle of *Streptomyces coelicolor*. *Int. J. Med. Microbiol.* **305**, 183–189.

Tang, J., Luo, M., Niu, S., Zhou, H., Cai, X., Zhang, W., Hu, Y., Yin, Y., Huang, A., and Wang, D. 2010. The crystal structure of hexamer RraA from *Pseudomonas aeruginosa* reveals six conserved protein-protein interaction sites. *Protein J.* **29**, 583–590.

Yeom, J.H., Go, H., Shin, E., Kim, H.L., Han, S.H., Moore, C.J., Bae, J., and Lee, K. 2008. Inhibitory effects of RraA and RraB on RNAse E-related enzymes imply conserved functions in the regulated enzymatic cleavage of RNA. *FEMS Microbiol. Lett.* **285**, 10–15.